

## Original Article

# The role of pterostilbene in treating aged related macular degeneration and mechanism study

Wenbo Zhao, Kunbei Lai, Lijun Zhou, Fabao Xu, Chenjin Jin

Zhongshan Ophthalmic Center, Sun Yat-sen University, Guangzhou, China

Received October 11, 2016; Accepted November 29, 2016; Epub February 15, 2017; Published February 28, 2017

**Abstract:** Aged related macular degeneration (AMD) is one progressive eye disease with complicated pathogenesis mechanisms. The degeneration of retinal pigment epithelium (RPE) is the major pathological change of AMD, due to their gradual oxidation by free radicals. Pterostilbene as one derivative of resveratrol, has potent anti-oxidation function, but with unknown effects on AMD. This study aimed to investigate the function and mechanism of pterostilbene on RPE in AMD, further illustrating its effects on AMD, in order to provide evidences for clinical treatment of AMD. Mouse AMD model was established for separation and culture of RPE cells. Histological changes of AMD in mice were observed by electron microscope. 2 mM pterostilbene was added for 48 h treatment. MTT assay was used to test cell proliferation, whilst ELISA was employed to quantify expression of inflammatory factors TNF- $\alpha$  and IL-1 $\beta$ . Western blot was used to test VEGF protein expression. ROS contents, GSH and SOD activity were further analyzed. Analysis of pterostilbene pharmacodynamic parameters was conducted. Our result showed that the deposits were accumulated in RPE cells, the proliferation of which in AMD model mice was inhibited, accompanied with enhanced TNF- $\alpha$  and IL-1 $\beta$  expression, plus higher VEGF protein expression, ROS production, and lower GSH or SOD activity ( $P < 0.05$  compared to control group). The GSH and SOD pharmacodynamic parameters in group treated with Pterostilbene exhibited significant difference, compared to that in control ( $P < 0.05$ ). Pterostilbene treatment facilitated RPE cell proliferation, decreased TNF- $\alpha$  and IL-1 $\beta$  expression, inhibited VEGF expression, decreased ROS production, and elevated GSH and SOD activity ( $P < 0.05$  compared to model group). Pterostilbene can modulate oxidation-anti-oxidation balance via alleviating inflammation, and can inhibit VEGF expression while facilitate RPE cell proliferation in AMD, thus retarding AMD progression.

**Keywords:** Aged related macular degeneration, retinal pigment epithelium, pterostilbene, VEGF, inflammatory factor

## Introduction

Aged related macular degeneration (AMD) frequently occurs in middle-aged people over 50 years. As one progressive eye disease, it can eventually cause unilateral or bilateral blindness [1]. Age is one high risk factor for AMD. With aged population worldwide, incidence and mortality of AMD gradually increased by years [2]. AMD has complicated pathogenesis mechanism with unclear factors. Most studies agreed that both age and genetic factors were strongly correlated with AMD, whilst inflammation, oxidative stress, obesity and cardiovascular disease can all lead to AMD occurrence [3, 4]. Pathological features of AMD involve peripheral nerve and retinal lesion, including typical Bruch's membrane thickening, pigment precipi-

tation of retinal pigment epithelium (RPE), abnormality of choroid plexus, and vascularization of newly formed vessels in choroid plexus, among which RPE degeneration is the major pathological change [5, 6]. Derived from neuroectoderm, RPE cells can provide metabolic supporting for photo sensory cells. Abnormality of RPE cells can cause the loss of normal physiological functions, further causing precipitation in retina and AMD occurrence [7]. Under normal conditions, anti-oxidation defense system consisting of small molecule anti-oxidant, anti-oxidase and DNA repair system can maintain body redox homeostasis and clear reactive oxygen species (ROS) produced by the body. When redox homeostasis is interrupted, over-expression or inability for elimination of ROS cause oxidative stress response of cells [8]. The inabil-

ity of the body to clear excess ROS leads to cell damage, and accelerates ageing process. Therefore oxidative stress plays important roles in various aged-related diseases [9, 10]. The gradual oxidation of RPE by free radicals is one of its pathogenesis mechanism. Therefore the effective clearance of oxygen free radicals, maintaining body's oxidation/anti-oxidation balance is one major challenge in AMD prevention and treatment [11].

As one homologous derivative of resveratrol, pterostilbene has multiple functions including anti-oxidation, anti-bacterial, anti-tumor, regulating vasodilation, inhibiting platelet coagulation and mediating lipoprotein metabolism, thus can elevate body immune defense function [12-15]. Pterostilbene is one type of non-flavone polyphenol compound that is widely distributed in grape, nut, strawberry, resina draconis and propolis [14]. Current study has demonstrated the treatment efficacy of pterostilbene in treating Alzheimer's disease, cardiovascular disorder, brain trauma, tumor and hypercholesterolemia [15, 16]. Its effects on AMD, however, has not been studied. This research thus investigated the role and mechanism of pterostilbene on RPE of AMD, further illustrating the effect of pterostilbene on AMD, in order to provide evidences for clinical treatment of AMD.

### Materials and methods

#### *Experimental animals*

Healthy female C57BL/6 mice (age 6-7 weeks, SPF grade, body weight  $27\pm 5$  g) were purchased from Laboratory Animal Center of Sun Yat-sen University and were kept in an SPF grade facility with fixed temperature ( $21\pm 1^\circ\text{C}$ ) and humidity (50~70%) with 12/12 light/dark cycle.

Rats were used for all experiments, and all procedures were approved by the Animal Ethics Committee of Zhongshan Ophthalmic Center, Sun Yat-sen University.

#### *Equipment and reagent*

Hydroquinol was purchased from Sigma (US). Pterostilbene (98% purity) was purchased from Fujitsu (Japan). DMSO and MTT powders were purchased from Gibco (US). Trypsin-EDTA lysis

buffer was purchased from Sigma (US). PVDF membrane were purchased from Pall Life Sciences (US). EDTA was purchased from Hyclone (US). ELISA kit for TNF- $\alpha$  and IL-1 $\beta$  were purchased from R&D (US). SOD activity assay kit was purchased from Jiancheng (China). GSH test kit was purchased from Trevigen (US). Western blotting reagent was purchased from Beyotime (China). ECL reagent was purchased from Amersham Biosciences (US). Rabbit anti-mouse VEGF monoclonal antibody, and goat anti-rabbit horseradish peroxidase (HRP)-conjugated IgG secondary antibody were all purchased from Cell Signaling (US). Other common reagents were purchased from Sangon (China). Labsystem Version 1.3.1 microplate reader was purchased from Bio-rad (US). Ultrapure workstation was purchased from Suta (China).

#### *Animal grouping and treatment*

Healthy male C57BL/6 mice were randomly assigned into two groups (N=20 each), including control group and AMD model group.

#### *Mouse AMD model preparation*

Based on previous records [17], mice in the model group was fed using 8 g/L hydroquinol, using normal diet containing protein, vitamin, lipid, linoleic acid and taurine. Normal mice received normal diet without hydroquinol. The model preparation was carried out for 5 months.

#### *Histological changes by electron microscope*

Rats were killed (3 rats in each group), and the eyes were enucleated, before the fixation with 2.5% paraformaldehyde and glutaric acid mixed stationary liquid for 24 h. The cornea, lens and vitreous body tissue were removed, and then the 4 mm  $\times$  2 mm ball wall was cut for the fixation with osmic acid and glutaric acid mixture. The sample was embedded in epoxy resin and sectioned by using thin slice machine (LEICA ULTRACUT R type) (Leica, Germany). Transmission electron microscopy (JEM1010EX) (JEOL, Japan) was employed for observation.

#### *RPE cell culture*

Control and model rats were anesthetized by 2% lidocaine via post-bulbar injection. Bilateral

eyeballs were removed under sterile conditions. Attached fascia tissues were removed. The eyeball was rinsed in gentamicin-containing saline and was placed in DMEM culture medium. A circular incision was made 3 mm posterior of corneoscleral junction. Anterior segment and viscous body were removed, followed by 0.25% trypsin digestion for 10 min. Retinal neural epithelial layer was separated and removed. Remaining eyecup, which contained RPE cell layer, was cut radically. After 0.25% trypsin digestion for 30 min at 37°C. Cells suspensions were then centrifuged at 800 rpm for 10 min. the supernatant was discarded and cultured medium containing 100 U/ml penicillin and 100 µg/ml streptomycin was added for incubation at 37°C with 5% CO<sub>2</sub>. Culture medium was changed every changed every other day. Cells were passed every 2-3 days. RPE cells at log-growth phase at 2<sup>nd</sup> to 8<sup>th</sup> generation were used for experiments. Model group was randomly divided into two groups: control group; and pterostilbene group, which received 2.0 mmol/L pterostilbene treatment for 48 h as previously recorded [18].

### *MTT assay for RPEs cell growth*

RPE cells at log-phase were digested, counted and seeded into 96-well plate at 3000 cells per well. Cells were randomly assigned into three groups: normal control group, model group and pterostilbene group (N=5). After 48-hour incubation, 20 µl MTT solution (5 g/L) was then added into each test well. With 4 h continuous culture, the supernatant was completely removed, with the addition of 150 µl DMSO for 10 min vortex until the complete resolving of crystal violet. Absorbance (A) values was measured at 570 nm in a microplate reader. The proliferation rate was calculated in each group. Each experiment was repeated in triplicates for statistical analysis.

### *ELISA for inflammatory factor TNF-α and IL-1β expression*

Cell culture supernatant was collected and tested for expression levels of TNF-α and IL-1β following the manual instruction of test kits. In brief, 96-well plate was added with 50 µl serially diluted samples, which were used to plot standard curves. 50 µl test samples were then added into test wells in triplicates. After washing for 5 times, liquids were discarded to fill

with washing buffer for 30 sec vortex. The rinsing procedure was repeated for 5 times. 50 µl enzyme labelling reagent was then added into each well except blank control. After gentle mixture, the well was incubated for 30 min at 37°C. Chromogenic substrates A and B were sequentially added (50 µl each), followed by 37°C dark incubation for 10 min. The test plate was then mixed with 50 µl quenching buffer as the blue color turned into yellow. Using blank control well as the reference, absorbance (A) values at 450 nm wavelength were measured by a microplate reader within 15 min after adding quenching buffer. Linear regression model was then plotted based on the concentration of standard samples and respective A values. Sample concentration was further deduced based on A values and regression function.

### *Pterostilbene pharmacodynamics*

The elimination rate constant of GSH and SOD (Ke), the elimination effect of half-life [t<sub>1/2</sub> (Ke)], the effect emerging rate constant (Ka), the effect presenting half-life [t<sub>1/2</sub> (Ke)], the duration of the effect (tm), peak time of effect (tp) were calculated.

### *Western blot for VEGF protein expression*

Proteins were extracted from RPE cells. In brief, tissues were mixed with lysis buffer for 15~30 min iced incubation. Using ultrasonic rupture (5 s, 4 times) and centrifugation (10000 g, 15 min), proteins were quantified from the supernatant and were kept at -20°C for Western blotting. Proteins were separated in 10% SDS-PAGE, and were transferred to PVDF membrane by semi-dry method. Non-specific binding sites were blocked by 5% defatted milk powders for 2 hours. Anti-VEGF monoclonal antibody (1:1000) was applied for 4°C overnight incubation. Goat anti-rabbit IgG (1:2000) was then added for 30-min incubation. After PBST washing and ECL development for 1 min, the membrane was exposed under X-ray. An imaging analyzing system and Quantity one software were then used to scan X-ray films and to detect the density of bands with repeated measures (N=4).

### *SOD activity in cells*

Using SOD activity assay kit, SOD activity was tested in RPE cells following manual instruc-

## Anti-oxidation in AMD

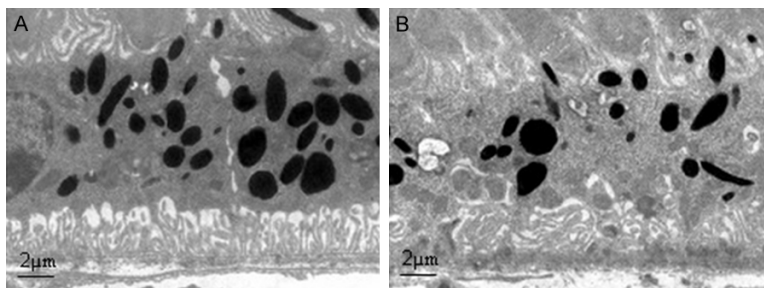


**Figure 1.** Histological changes of AMD by electron microscope ( $\times 10000$ ). A: Control groups; B: Model group.

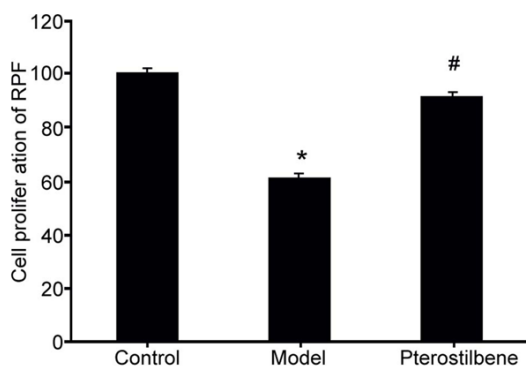


**Figure 2.** Effects of pterostilbene on RPEs cell proliferation in AMD mice. \* $P < 0.05$  compared to control group; # $P < 0.05$  compared to model group.

tion. In brief, cell proteins extracted were denatured at  $95^{\circ}\text{C}$  for 40 min, and were centrifuged at 4000 rpm for 10 min after cooling down. Ethanol-chloroform mixture (5:3, v/v) was used to extract ethanol phase in the homogenate for total SDO activity assay.

### ROS content assay in cells

Cells were denatured at  $95^{\circ}\text{C}$  for 40 min, rinsed in cold water, and were centrifuged at 4000 rpm for 10 min. At  $37^{\circ}\text{C}$ , homogenates were incubated in 2', 7'-dichlorofluorescein diacetate (DCF-DA) for 15 min. After centrifugation at 10000 rpm for 15 min, precipitations were re-suspended in sterilized PBS buffer, and were incubated at  $37^{\circ}\text{C}$  for 60 min. Spectrometry was used to detect the ROS levels expressed as ROS production percentage.

### GSH content assay

Cells were homogenized in vortex and were denatured at  $95^{\circ}\text{C}$  for 40 min, rinsed in cold water, and were centrifuged at 4000 rpm for 10 min. Following the manual instruction of GSH

assay kit, cell supernatant was mixed with 5% phosphorous acid, followed by 4000 rpm centrifugation for 10 min. Total supernatant was collected for detecting GSH level change. The mixture was incubated for 5 min, and was tested for GSH activity change at 420 nm wavelength. The concentration of GSH was measured based on standard curve of GSH. At 1.0 cm photo-diameter, OD value was measured by colorimetry. GSH result was presented as nmol content in each mg protein.

photo-diameter, OD value was measured by colorimetry. GSH result was presented as nmol content in each mg protein.

### Statistical analysis

SPSS16.0 software was used for data analysis. Measurement data were presented as mean  $\pm$  standard deviation (SD). One-way analysis of variance (ANOVA) was employed for comparing between multiple groups. Post-hoc test following ANOVA (tamhane's T2) was conducted for multiple comparisons between groups as equal variance was not assumed. A statistical significance was defined when  $P < 0.05$ .

## Results

### The observation of histological changes

The result of AMD by electron microscope showed that RPE cell in the control group presented integral structure, long microvilli, orderly arranged basal infolding, plenty of mitochondria, with similar thickness. In the model group, however, RPE cells exhibited incomplete structure, short microvilli, vacuolized mitochondrial, layered sediments in outer layer collagen (**Figure 1**).

### Effects of pterostilbene on RPEs cell proliferation in AMD

MTT assay was used to test the effect of pterostilbene on RPE cell proliferation in AMD model mice. Results showed significantly inhibited proliferation of RPE cells in AMD model mice ( $P < 0.05$  compare to normal control group). Pterostilbene treatment significantly facilitated RPE cell proliferation in AMD mice ( $P < 0.05$  compared to model group, **Figure 2**). These above results indicated that pterostilbene could facilitate proliferation of RPE cells in AMD model mice.

## Anti-oxidation in AMD

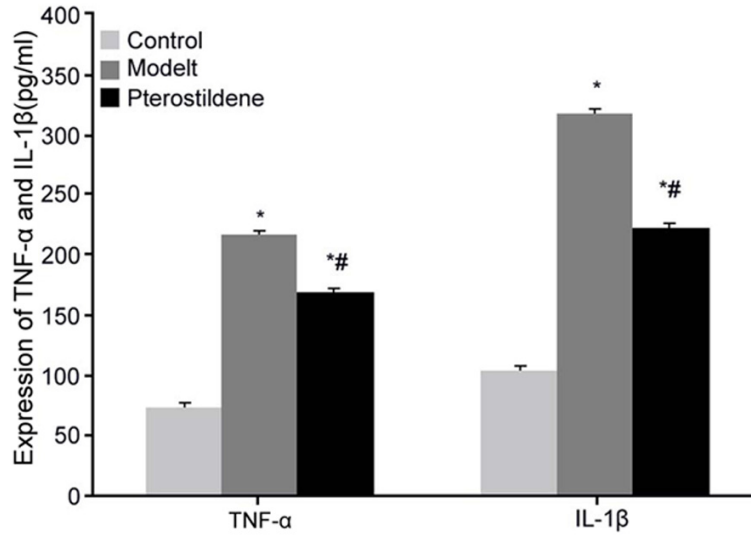


**Figure 3.** Effects of pterostilbene on inflammatory factors TNF- $\alpha$  and IL-1 $\beta$  in AMD mice. \*P<0.05 compared to control group; #P<0.05 compared to model group.

and IL-1 $\beta$  expression in RPEs supernatant of AMD model mice (P<0.05 compared to normal control group). Pterostilbene treatment significantly inhibited TNF- $\alpha$  and IL-1 $\beta$  expression in RPEs supernatant (P<0.05 compared to model group, **Figure 3**) but was still higher than those of normal control group (P<0.05). These above results suggested that pterostilbene could decrease secretion of inflammatory factors in RPE cells of AMD mice, thus alleviating inflammatory response.

### *Effects of pterostilbene on VEGF protein expression of AMD mice*

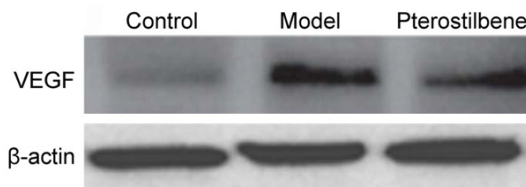


**Figure 4.** Effects of pterostilbene on VEGF protein expression in AMD mice.

Western blot was used to test the effect of pterostilbene on expression of VEGF protein in RPE cells of AMD mice. Results showed enhanced VEGF protein expression in RPEs cells of AMD model mice (P<0.05 compared to normal control group). Pterostilbene treatment significantly inhibited VEGF proteins in RPEs cells (P<0.05 compared to model group, **Figures 4 and 5**). These results suggested that pterostilbene could facilitate VEGF expression, leading to AMD pathogenesis. Pterostilbene could exert effects on AMD RPE cells, thus depressing VEGF protein expression.

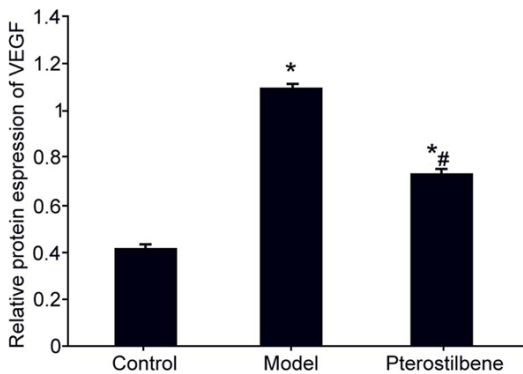


**Figure 5.** Analysis of pterostilbene effect on VEGF protein expression in AMD mice. \*P<0.05 compared to control group; #P<0.05 compared to model group.

### *Effects of pterostilbene on ROS content of RPE cells*

ROS production levels in all groups of cells were tested. Results showed significantly enhanced ROS production in RPEs cells (P<0.05 compared to control group). Pterostilbene treatment on RPE cells significantly inhibited ROS production (P<0.05 compared to model group, **Figure 6**).

### *Effects of pterostilbene on SOD activity in RPE cells*

SOD activities in all groups of cells were tested. Results showed significantly lower SOD activity in RPEs cells (P<0.05 compared to control group). Pterostilbene treatment on RPE cells significantly enhanced SOD activity in RPE cells (P<0.05 compared to model group, **Figure 7**).

### *Effects of pterostilbene on inflammatory factors TNF-α and IL-1β in AMD mice*

ELISA was used to test the effect of pterostilbene on expression of inflammatory factors TNF- $\alpha$  and IL-1 $\beta$  in RPE cell supernatant. Results showed significantly elevated TNF- $\alpha$

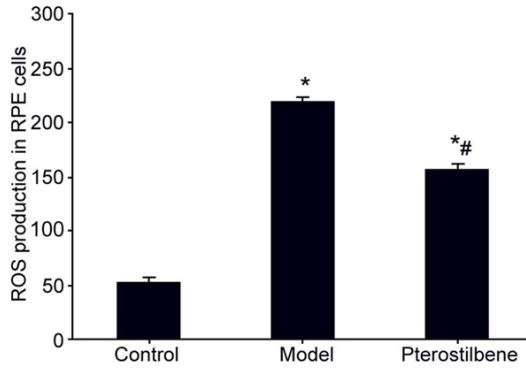


**Figure 6.** Effects of pterostilbene on ROS contents of RPE cells. \*P<0.05 compared to control group; #P<0.05 compared to model group.

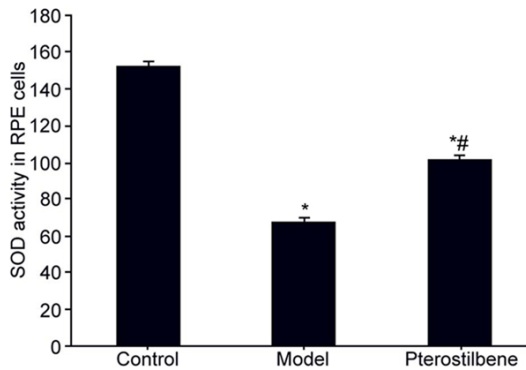


**Figure 7.** Effects of pterostilbene on SOD activity of RPE cells. \*P<0.05 compared to control group; #P<0.05 compared to model group.

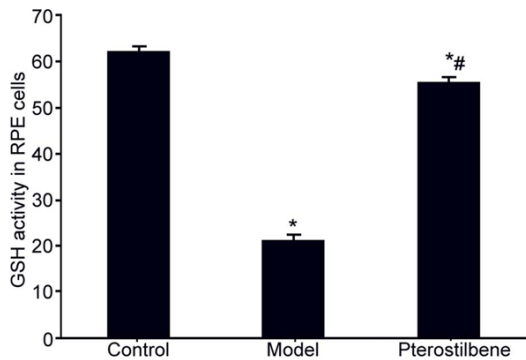


**Figure 8.** Effects of pterostilbene on GSH activity of RPE cells. \*P<0.05 compared to control group; #P<0.05 compared to model group.

*Effects of pterostilbene on GSH activity of RPE cells*

GSH activity in all groups of cells was tested. Results showed significantly lower GSH activity

**Table 1.** The pharmacodynamics parameters of pterostilbene on GSH and SOD

	GSH	SOD
Ke	0.00063	0.00221
Ka	0.1041	0.1710
$t_{1/2 (Ke)}$	1091.33	310.85
$t_{1/2 (Ka)}$	6.68	4.05
$t_p$	42.18	25.93

in RPEs cells of AMD model mice (P<0.05 compared to control group). Pterostilbene treatment on RPE cells significantly enhanced GSH activity (P<0.05 compared to model group, **Figure 8**).

*Pharmacodynamics of pterostilbene*

In this study, we also detected the pharmacodynamic parameters in order to evaluate the effects of pterostilbene on GSH and SOD. The data of different impacts on GSH and SOD indicated that pterostilbene had potent antioxidant effect, with the profiles of high-strength and long-lasting effect (**Table 1**).

**Discussion**

During pathogenesis and progression of AMD, RPE cell injury is one early event, making the maintenance of normal structure and function of RPE critical for retarding AMD occurrence [19]. RPE cells are specialized tissues under the effect of ROS, with aggregation of photo sensory cells and pigment in macular region, further affecting vision. Therefore, eye is sensitive for light irradiation and photo-chemistry injury. With its high oxygen expenditure status, it can further participate in metabolism and phagocytosis functions [20]. When oxidative stress occurs, anti-oxidation defense system is compromised, enriching ROS, further aggravating AMD occurrence and progression [21]. This study thus established an AMD mouse model on which RPE cells were separated to find inhibited cell proliferation in AMD mice, accompanied with higher TNF- $\alpha$  and IL-1 $\beta$  expression levels, higher ROS production, lower GSH or SOD activity. Histological detection result also confirmed that RPE cells in model group presented obvious pathological changes, which is strictly associated with the occurrence and development of AMD.

Further study added pterostilbene on RPE cells of AMD model. Results showed that pterostilbene could facilitate RPE cell proliferation, decrease TNF- $\alpha$  and IL-1 $\beta$  expression or ROS production, and enhance GSH production and SOD activity. Pterostilbene is one metabolism of resveratrol with more potent pharmaceutical efficacy. Besides advantages in pharmaceutical functions, pterostilbene has highly selectivity. After forming its methylation product pterostilbene, resveratrol has highly biological activity and selectivity, plus lower toxicity, making more application advantages over resveratrol. Pterostilbene still has important roles in anti-inflammation and regulating redox homeostasis [15, 16]. Our pharmacodynamic analysis also unraveled high values of parameters in SOD than that in GSH, suggesting a stronger effect of pterostilbene on SOD than that on GSH. Study showed that abundant ROS could injury mitochondrial and lysosomal structures inside RPE cells. Mitochondrial injury can produce more ROS inside the body, forming a vicious circle to induce cell apoptosis, abnormality in RPE cells, and shortening and disorder of photo sensory cells [22]. Anti-oxidase hydrogenase GSH and SOD can form anti-oxidants to effectively clear ROS, thus maintaining normal cell physiology mechanism and impeding oxidative stress injury on RPE cells [23]. During oxidative stress injury, both inflammatory and immune factors could induce AMD pathogenesis. The drusen produced by oxidative stress response precipitates between RPE cell layers, activating macrophage, enhancing inflammatory factor production. On the other hand, RPE cannot effectively absorb oxygen or nutrients under the influence of drusen, thus leading over-production of vascular endothelial cells and angiogenesis in choroid plexus [24, 25]. Therefore, AMD pathogenesis and inflammation are closely related with VEGF. This study demonstrated that pterostilbene could inhibit AMD inflammation, and decrease VEGF production, thus retarding AMD progression.

### Conclusion

Pterostilbene could facilitate RPE cell proliferation in AMD via alleviating inflammation, regulating oxidation/anti-oxidation balance and inhibiting VEGF expression, thus retarding AMD progression. Therefore, the re-establishment of anti-oxidase homeostasis can benefit the study of effective treatment for AMD.

### Disclosure of conflict of interest

None.

**Address correspondence to:** Dr. Chenjin Jin, Department of Zhongshan Ophthalmic Center, Sun Yat-sen University, 54 South Xianlie Road, Guangzhou 510000, China. Tel: +86-020-87331366; Fax: +86-020-87331366; E-mail: ChenjinJin889@163.com

### References

- [1] Hamade N, Hodge WG, Rakibuz-Zaman M and Malvankar-Mehta MS. The effects of low-vision rehabilitation on reading speed and depression in age related macular degeneration: a meta-analysis. *PLoS One* 2016; 11: e0159254.
- [2] Iroku-Malize T and Kirsch S. Eye Conditions in older adults: age-related macular degeneration. *FP Essent* 2016; 445: 24-8.
- [3] Gliem M, Muller PL, Finger RP, McGuinness MB, Holz FG and Charbel Issa P. Quantitative fundus autofluorescence in early and intermediate age-related macular degeneration. *JAMA Ophthalmol* 2016; 134: 817-24.
- [4] Saxena N, George PP, Hoon HB, Han LT and Onn YS. Burden of wet age-related macular degeneration and its economic implications in singapore in the year 2030. *Ophthalmic Epidemiol* 2016; 23: 232-7.
- [5] Aboelnour A, Kam JH, Elnasharty MA, Sayed-Ahmed A and Jeffery G. Amyloid beta deposition and phosphorylated tau accumulation are key features in aged choroidal vessels in the complement factor H knock out model of retinal degeneration. *Exp Eye Res* 2016; 147: 138-43.
- [6] Chen Y, Hahn P and Sloan FA. Changes in visual function in the elderly population in the United States: 1995-2010. *Ophthalmic Epidemiol* 2016; 23: 137-44.
- [7] Cymerman RM, Skolnick AH, Cole WJ, Nabati C, Curcio CA and Smith RT. Coronary artery disease and reticular macular disease, a subphenotype of early age-related macular degeneration. *Curr Eye Res* 2016; 41: 1482-1488.
- [8] Allingham MJ, Nie Q, Lad EM, Izatt DJ, Mettu PS, Cousins SW and Farsiu S. Semiautomatic segmentation of rim area focal hyperautofluorescence predicts progression of geographic atrophy due to dry age-related macular degeneration. *Invest Ophthalmol Vis Sci* 2016; 57: 2283-9.
- [9] Chang P, Tan A, Jaffe GJ, Fleckenstein M, Holz FG and Schmitz-Valckenberg S. Analysis of peripapillary atrophy in relation to macular geographic atrophy in age-related macular degeneration. *Invest Ophthalmol Vis Sci* 2016; 57: 2277-82.

- [10] Feng L, Cao L, Zhang Y and Wang F. Detecting Abeta deposition and RPE cell senescence in the retinas of SAMP8 mice. *Discov Med* 2016; 21: 149-58.
- [11] Acharya UR, Mookiah MR, Koh JE, Tan JH, Noronha K, Bhandary SV, Rao AK, Hagiwara Y, Chua CK and Laude A. Novel risk index for the identification of age-related macular degeneration using radon transform and DWT features. *Comput Biol Med* 2016; 73: 131-40.
- [12] Pan C, Hu Y, Li J, Wang Z, Huang J, Zhang S and Ding L. Estrogen receptor- $\alpha$ 36 is involved in pterostilbene-induced apoptosis and anti-proliferation in in vitro and in vivo breast cancer. *PLoS One* 2014; 9: e104459.
- [13] Saw CL, Guo Y, Yang AY, Paredes-Gonzalez X, Ramirez C, Pung D and Kong AN. The berry constituents quercetin, kaempferol, and pterostilbene synergistically attenuate reactive oxygen species: involvement of the Nrf2-ARE signaling pathway. *Food Chem Toxicol* 2014; 72: 303-11.
- [14] Wu X, Zhou S, Zhu N, Wang X, Jin W, Song X and Chen A. Resveratrol attenuates hypoxia/reoxygenation induced  $Ca^{2+}$  overload by inhibiting the Wnt5a/Frizzled2 pathway in rat H9c2 cells. *Mol Med Rep* 2014; 10: 2542-8.
- [15] Hou XL, Tong Q, Wang WQ, Shi CY, Xiong W, Chen J, Liu X and Fang JG. Suppression of Inflammatory responses by dihydromyricetin, a flavonoid from *Ampelopsis grossedentata*, via inhibiting the activation of NF- $\kappa$ B and MAPK signaling pathways. *J Nat Prod* 2015; 78: 1689-96.
- [16] Hannan PA, Khan JA, Ullah I and Ullah S. Synergistic combinatorial antihyperlipidemic study of selected natural antioxidants; modulatory effects on lipid profile and endogenous antioxidants. *Lipids Health Dis* 2016; 15: 151.
- [17] Pons M, Cousins SW, Csaky KG, Striker G and Marin-Castano ME. Cigarette smoke-related hydroquinone induces filamentous actin reorganization and heat shock protein 27 phosphorylation through p38 and extracellular signal-regulated kinase 1/2 in retinal pigment epithelium: implications for age-related macular degeneration. *Am J Pathol* 2010; 177: 1198-213.
- [18] Yoon HS, Hyun CG, Lee NH, Park SS and Shin DB. Comparative depigmentation effects of resveratrol and its two methyl analogues in alpha-melanocyte stimulating hormone-triggered B16/F10 murine melanoma cells. *Prev Nutr Food Sci* 2016; 21: 155-9.
- [19] Fu Y, Tang M, Bai L and Fan Y. The role of apoptosis inducing factor in the apoptosis of retinal pigment epithelium cells induced by oxidative stress. *Cell Mol Biol (Noisy-le-grand)* 2016; 62: 36-41.
- [20] Chong CM and Zheng W. Artemisinin protects human retinal pigment epithelial cells from hydrogen peroxide-induced oxidative damage through activation of ERK/CREB signaling. *Redox Biol* 2016; 9: 50-56.
- [21] Fu D, Yu JY, Connell AR, Yang S, Hookham MB, McLeese R and Lyons TJ. Beneficial effects of berberine on oxidized LDL-induced cytotoxicity to human retinal muller cells. *Invest Ophthalmol Vis Sci* 2016; 57: 3369-79.
- [22] Chan CM, Huang DY, Huang YP, Hsu SH, Kang LY, Shen CM and Lin WW. Methylglyoxal induces cell death through endoplasmic reticulum stress-associated ROS production and mitochondrial dysfunction. *J Cell Mol Med* 2016; 20: 1749-60.
- [23] Yang PM, Wu ZZ, Zhang YQ and Wung BS. Lycopene inhibits ICAM-1 expression and NF- $\kappa$ B activation by Nrf2-regulated cell redox state in human retinal pigment epithelial cells. *Life Sci* 2016; 155: 94-101.
- [24] Gupta D, Gupta V, Singh V, Prakash S, Agrawal S, Chawla S and Phadke SR. Vascular endothelial growth factor gene polymorphisms and association with age related macular degeneration in Indian patients. *Meta Gene* 2016; 9: 249-53.
- [25] Kim M, Kim ES, Seo KH, Yu SY and Kwak HW. Change of retinal pigment epithelial atrophy after anti-vascular endothelial growth factor treatment in exudative age-related macular degeneration. *Indian J Ophthalmol* 2016; 64: 427-33.